

# Wavelength control with grating imprinted fiber Sagnac loop mirror by polarization and strain tuning

Ping Lu,<sup>1</sup> Liqiu Men,<sup>2</sup> and Qiying Chen<sup>1,3,a)</sup>

<sup>1</sup>*Department of Physics and Physical Oceanography, Memorial University of Newfoundland, St. John's, Newfoundland A1B 3X7, Canada*

<sup>2</sup>*CREAIT Network, Memorial University of Newfoundland, St. John's, Newfoundland A1C 5S7, Canada*

<sup>3</sup>*Faculty of Engineering and Applied Science, Memorial University of Newfoundland, St. John's, Newfoundland A1B 3X5, Canada*

(Received 6 May 2009; accepted 8 June 2009; published online 15 July 2009)

Wavelength control by the use of fiber Bragg grating (FBG) imprinted polarization maintaining fiber (PMF) Sagnac loop mirror (SLM) is proposed and demonstrated through polarization and strain tuning. The Bragg wavelengths of the FBG in the PMF along slow or fast axis show redshifts with the increase in strain with sensitivities of  $8.77 \times 10^{-4}$  and  $9.11 \times 10^{-4}$  nm/ $\mu\epsilon$ , respectively, whereas the interferometric peak wavelength of the SLM exhibits a blueshift with a sensitivity of  $1.9437 \times 10^{-2}$  nm/ $\mu\epsilon$  for the peak with an order number of 420. The opposite strain sensitivities and the pronounced difference in the bandwidth of the FBG resonance peak and that of the SLM, together with the controllability on the wavelength spacing of the SLM neighboring transmission maxima, provide a variety of alternatives to realize wavelength tuning for many practical applications.

© 2009 American Institute of Physics. [DOI: [10.1063/1.3168435](https://doi.org/10.1063/1.3168435)]

## I. INTRODUCTION

Precise and stable wavelength control is one of the key technologies to achieve the ultimate spectral efficiency and maximize the system capacity for telecommunication networks, and to realize controllability and optimization of laser frequencies in many test and measurement systems.<sup>1</sup> Examples include high-power wavelength stabilized semiconductor pump lasers in erbium doped fiber amplifiers and Raman fiber amplifiers,<sup>2</sup> wavelength division multiplexers,<sup>3</sup> and multiwavelength fiber lasers.<sup>4,5</sup> In many applications, spectral filtering is a critical requirement, for which several techniques have been reported, including optical thin film interference filters,<sup>6</sup> ultranarrow optical filtering based on fiber Bragg gratings (FBGs),<sup>7</sup> and volume Bragg grating as a spectral selective reflective element.<sup>8</sup> Notably FBGs have been recognized as powerful wavelength-selective components in fiber-optic systems. As a special case of spectral filtering, wavelength locking by the use of a FBG to lock the output from a semiconductor laser at a single wavelength has been reported.<sup>2,9</sup> However, the polarization properties of the lasers are ignored in all these techniques.

Recently, a fiber Sagnac loop mirror (SLM) incorporating polarization maintaining fiber (PMF) has attracted considerable attention as an optical comb filter due to its intrinsic merits such as low insertion loss, polarization independence to input light, broad useful spectral bandwidth, and high resistance to environmental changes.<sup>4,10-13</sup> Most of the optical comb filters reported so far lack flexibility, except that some of them are tunable in the absolute position of the output or the channel space with the use of specialty fibers or complicated configurations.<sup>4,10,14</sup> The comb filter can be tuned by changing the operating temperature of the SLM

using a pumped erbium-ytterbium codoped PMF,<sup>4</sup> high-birefringence elliptical core side-hole fiber,<sup>10</sup> PANDA PMF from our recent work,<sup>15</sup> or additional active devices in the fiber loop mirror.<sup>16</sup> A SLM based on a polarization maintaining photonic crystal fiber with reduced temperature sensitivity was also reported.<sup>12</sup>

In this letter, we propose and experimentally demonstrate an approach to achieve wavelength control with a fiber Bragg grating imprinted polarization maintaining fiber (PMFBG) SLM through polarization and strain tuning. The combination of a FBG and a fiber loop mirror realizes switching of the transmission spectrum from a narrow PMFBG filter to a SLM comb filter. The opposite strain sensitivities of the Bragg wavelengths of the FBG and the interferometric peaks of the loop mirror provide an opportunity to achieve wavelength selectivity. In addition to the versatility in the selections of the Bragg wavelength of a FBG and the interferometric peaks of a loop mirror to satisfy specific applications, the realization of the technique on a standard PANDA fiber provides an easy and low-cost approach, which is compatible with the existing fiber-optic systems.

## II. EXPERIMENTAL DETAILS

The operation principle to realize wavelength control with Bragg grating imprinted PMF is basically a SLM with a broadband light source (EBS-7210, MPB Communications, Inc.) and the detection of the interference signal using an optical spectrum analyzer (OSA) (Ando AQ6315E). As shown in Fig. 1, broadband light is launched into a single-mode 50:50 fiber coupler and divided into two arms where beams propagate either clockwise or counterclockwise. A SLM is formed when a polarization controller (HP 11896A) and a 10 cm FBG inscribed PMF (PANDA, Thorlabs) of 210 cm in length connect the two ends of the fiber coupler. Details on the fabrication of the FBG can be found elsewhere.<sup>17</sup> The reflection spectrum of the FBG is detected by the OSA,

<sup>a)</sup>Author to whom correspondence should be addressed. Electronic mail: [qiyingc@mun.ca](mailto:qiyingc@mun.ca).

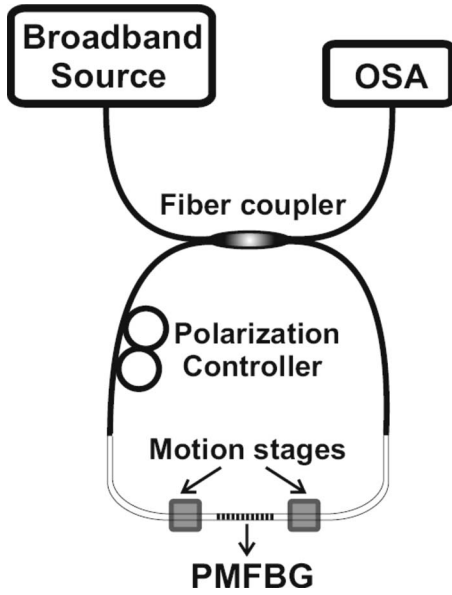


FIG. 1. Schematic illustration of the experimental setup.

which shows the fast-axis Bragg resonance wavelength at 1546.073 nm with a reflection of 3.20 dB and the slow-axis Bragg resonance wavelength at 1546.440 nm with a reflection of 4.59 dB (Fig. 2).

### III. RESULTS AND DISCUSSION

The FBG imprinted in the SLM serves as a reflector only at the Bragg resonance wavelengths, which does not affect the other wavelength regions where the Sagnac interference forms in the fiber coupler. The optical intensity transmission spectrum  $T(\lambda)$  of the SLM can be calculated using the Jones matrix method with an expression<sup>14,18</sup>

$$T(\lambda) = \cos^2\left(\frac{\pi LB}{\lambda}\right) \cos^2 \theta, \tag{1}$$

where  $L$ ,  $B$ , and  $\lambda$  are the length, the birefringence, and the operation wavelength of the PMF, respectively.  $\theta$  is the angle

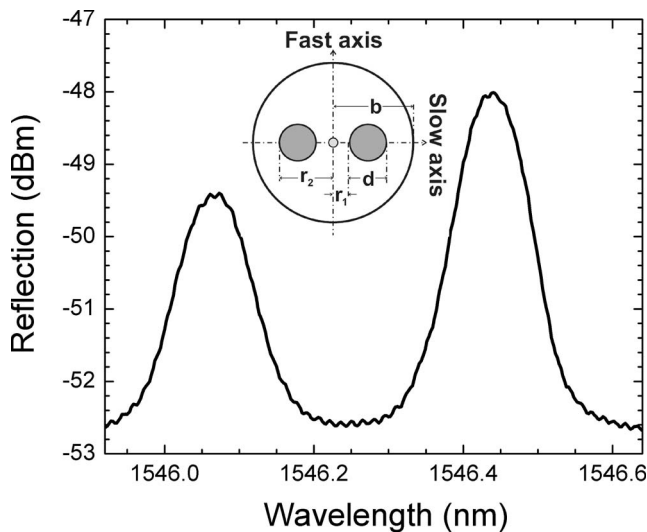


FIG. 2. Reflection spectrum of the PMFBG. The inset shows the cross section of a PANDA fiber.

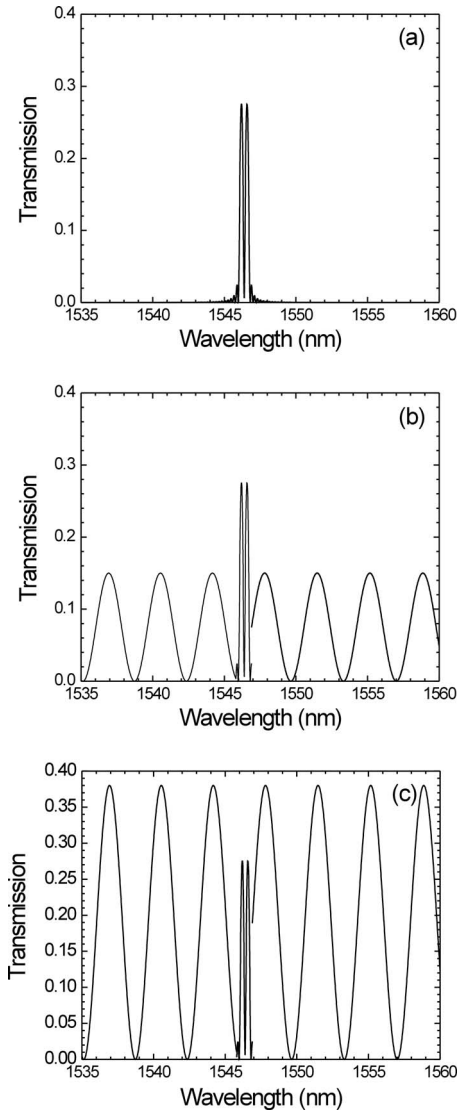


FIG. 3. Simulated transmission spectra of the PMFBG in the SLM at different polarization states: (a) 90°, (b) 70°, and (c) 50°.

between the input light and the fast axis of the PMF.

When the polarization controller is set to produce input light of different polarization states, the transmission spectrum of the PMFBG superimposed SLM will change accordingly. The simulated transmission spectra of the PMFBG in the SLM at different polarization states are shown in Fig. 3. At  $\theta=90^\circ$ , the transmitted output of the filter is zero except that the resonance peaks of the PMFBG appear in the spectrum, which is a narrow PMFBG filter. At  $\theta=50^\circ$ , the interference intensity of the SLM increases and exceeds that of the PMFBG, forming a comb filter. At  $\theta=70^\circ$ , the PMFBG resonance peaks are superimposed on the SLM interferometric pattern. Figure 4 shows the experimental observation of the transmission spectrum changed from a narrow PMFBG filter to a SLM comb filter by adjusting the polarization controller. The experimental results are consistent with the theoretical analysis.

When the axial strain changes from an initial value of  $\epsilon_0$  to  $\epsilon$  along a segment of the PMFBG with a length of  $l$ , a second-order Taylor series expansion around  $\epsilon_0=0$  can be derived from Eq. (1) as

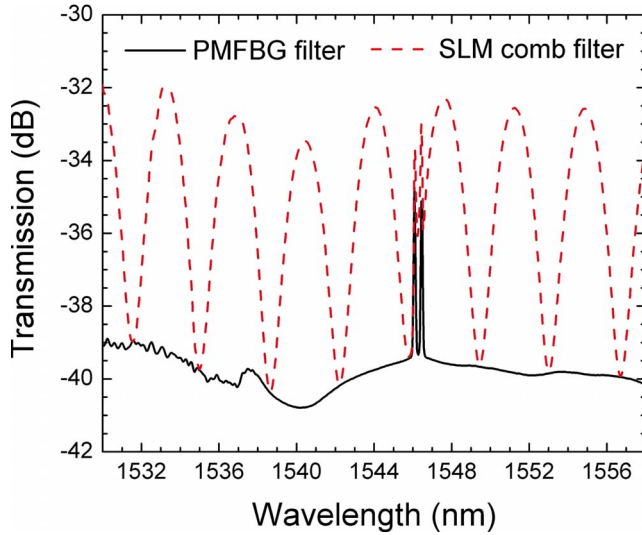


FIG. 4. (Color online) Transmission spectrum switching from a narrow PMFBG filter to a SLM comb filter by adjusting the polarization controller.

$$T(\lambda) \approx \cos^2 \left[ \frac{\pi[(L-l) + l(1+\varepsilon)]}{\lambda} \left( B(0) + \frac{dB(\varepsilon)}{d\varepsilon} \varepsilon \right) \right] \\ = \cos^2 \left( \frac{\pi(L+l\varepsilon)}{\lambda} B(0) + \frac{\pi l(1+\varepsilon)\varepsilon}{\lambda} \frac{dB(\varepsilon)}{d\varepsilon} \right). \quad (2)$$

From Eq. (2), the SLM peak wavelength requires

$$\lambda_k = \frac{(L+l\varepsilon)B(0)}{k} + \frac{(l+l\varepsilon)\varepsilon}{k} \frac{dB}{d\varepsilon}. \quad (3)$$

Thus the gradient of the SLM peak wavelength due to the changes in the longitudinal strain and the corresponding change in the birefringence is

$$\frac{d\lambda_k}{d\varepsilon} = \frac{lB(0)}{k} + \left[ \frac{l}{k} \frac{dB}{d\varepsilon} + \frac{l\varepsilon}{k} \frac{d^2B}{d\varepsilon^2} \right] + \left[ \frac{2l\varepsilon}{k} \frac{dB}{d\varepsilon} + \frac{l\varepsilon^2}{k} \frac{d^2B}{d\varepsilon^2} \right]. \quad (4)$$

The birefringence  $B$  of the PMF can be expressed as  $B = n_S - n_F$ , where  $n_S$  and  $n_F$  are the effective refractive indices corresponding to the slow axis and the fast axis of the PMF, respectively. The parameter  $B$  of a PMF is given by<sup>19</sup>

$$B = B_G + B_{S_0} + B_S, \quad (5)$$

where  $B_G$  is the geometrical component,  $B_{S_0}$  is the self-stress component, and  $B_S$  is the outer stress component. In the PANDA fiber, the modal birefringence components  $B_G$  and  $B_{S_0}$  are zero.  $B_S$  can be expressed as

$$B_S = \frac{\alpha_T(T - T_S)n_1^3(P_{11} - P_{12})(1 + \nu)(r_2 - r_1)}{(1 - \nu^2)(r_2 + r_1)} \\ \times \left\{ 1 - \frac{3}{b^4}(r_2 - r_1)^4 \right\}, \quad (6)$$

where  $T$  is the environmental temperature around the fiber,  $r_1$  and  $r_2$  are the corresponding inner and outer radii of the stress-applying parts to the fiber core,  $b$  is the outer cladding radius, and all the other parameters are constants. The inset of Fig. 2 illustrates the cross section of a PANDA fiber where

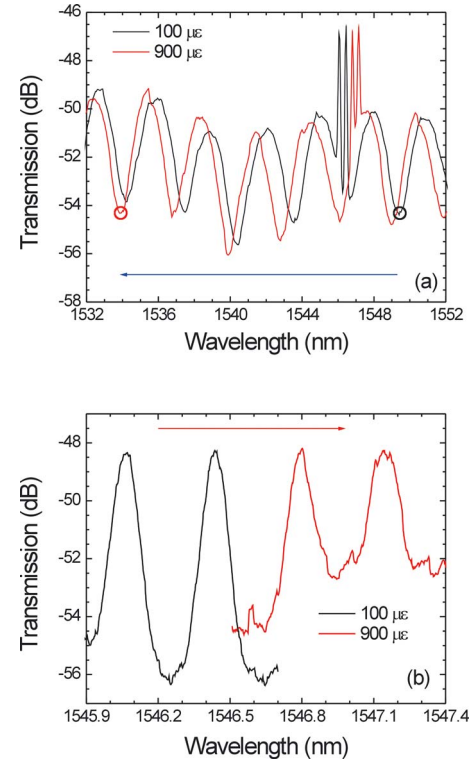


FIG. 5. (Color online) Transmission spectra from an axial strain of 100–900 $\mu\varepsilon$ : (a) blueshifting spectra of the PMFBG imprinted fiber SLM and (b) redshifting spectra of the PMFBG.

the diameter of the stress-applying part is denoted by  $d$ .

If the parameters of the stress-applying part,  $r_1$ ,  $r_2$ , and  $d$ , are assumed unchanged when the PMF is axially stretched from  $l$  to  $l + \Delta l$ , the outer cladding radius will change from  $b$  to  $b'$  as

$$b' = b \sqrt{\frac{l}{l + \Delta l}} = b \sqrt{\frac{1}{1 + \varepsilon}}. \quad (7)$$

Following Eq. (6), the birefringence  $B(\varepsilon)$  of a PANDA PMF in an environment of constant temperature can be written as

$$B(\varepsilon) = c_1 \left( 1 - \frac{3d^4}{b'^4} \right) = c_1 \left( 1 - \frac{3(1 + \varepsilon)^2 d^4}{b^4} \right) \\ = -c_0(1 + \varepsilon)^2 + c_1, \quad (8)$$

where  $c_0$  and  $c_1$  are positive constants. For an environmental temperature of 20 °C,  $c_0$  and  $c_1$  are calculated to be  $9.57 \times 10^{-5}$  and  $4.64 \times 10^{-4}$ , respectively.

Through adjusting the polarization controller, the PMFBG resonance peaks were superimposed on the SLM interferometric pattern. The axial strain on a length of 40 cm PMF with the PMFBG in the center was changed from  $0\mu\varepsilon$  to  $1000\mu\varepsilon$  while the temperature was kept at room temperature of 20 °C. Figure 5 shows the transmission spectra of the PMFBG SLM with the axial strain changing from  $100\mu\varepsilon$  to  $900\mu\varepsilon$ . When a grating is inscribed in a PMF, two Bragg resonance wavelengths corresponding to the slow and fast axes of the FBG, i.e.,  $\lambda_S$  and  $\lambda_F$ , are dependent on the refractive index ( $n_S$  or  $n_F$ ) and the grating period ( $\Lambda_{\text{FBG}}$ ) following the relationship  $\lambda_{S,F} = 2n_{S,F}\Lambda_{\text{FBG}}$ .<sup>20</sup> As shown in Fig. 5(b), the slow-axis and fast-axis Bragg wavelengths of the FBG ex-

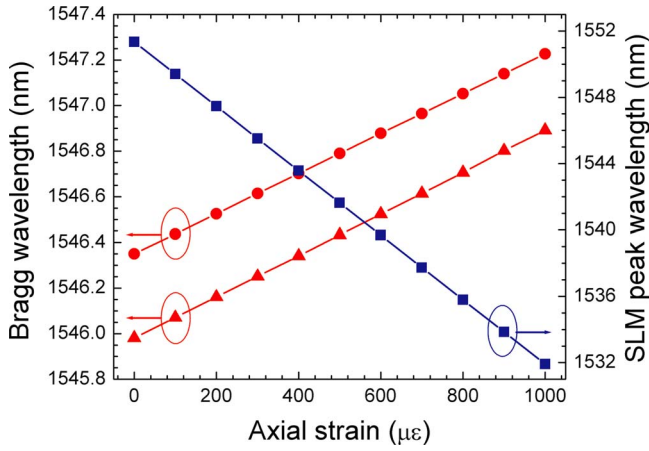


FIG. 6. (Color online) Axial strain dependences of the PMFBG SLM. The dots and the triangles stand for the Bragg resonance wavelengths of the slow axis and the fast axis as functions of the axial strain, respectively. The squares represent the interferometric peak wavelength of the fiber SLM as a function of axial strain for  $k=420$ .

hibit redshifts from 1546.437 and 1546.071 nm to 1547.140 and 1546.802 nm, respectively. However, the difference in their Bragg wavelengths decreases from 0.366 to 0.338 nm, which is due to the decrease in the birefringence of the fiber with the increasing axial strain as manifested in Eq. (8). When the applied strain increases from  $100\mu\epsilon$  to  $900\mu\epsilon$ , the SLM peak wavelength of 1549.400 nm, corresponding to the order number  $k=420$ , blueshifts to 1533.850 nm with a wavelength shift of 15.550 nm as shown in Fig. 5(a). Equation (4) can be rewritten with Eq. (8) as

$$\frac{d\lambda_k}{d\epsilon} = \frac{lB(0)}{k} - \frac{2c_0l}{k}(1 + 4\epsilon + 3\epsilon^2) \approx \frac{lB(0)}{k} - \frac{2c_0l}{k}, \quad (9)$$

where the birefringence of the PANDA fiber used in this study,  $B(0)$ , is calculated to be  $3.68 \times 10^{-4}$ .

Since the higher order strain effect on the birefringence can be neglected for an axial strain value of  $\sim 10^{-3}$ , the SLM peak wavelength responds linearly to a small axial strain. Furthermore, it is noted that the interference peak wavelengths of different mode numbers experience different changes under the same change in the axial strain, whereas the interference peak wavelength of a smaller mode number possesses a larger wavelength gradient.

When the applied axial strain is changed from  $0\mu\epsilon$  to  $1000\mu\epsilon$ , the Bragg resonance wavelengths of the PMFBG as functions of the increasing axial strain are shown in Fig. 6. The Bragg resonance wavelengths redshift linearly with the increasing axial strain with the axial strain sensitivities of  $8.77 \times 10^{-4}$  and  $9.11 \times 10^{-4}$  nm/ $\mu\epsilon$  for the Bragg resonance wavelengths along the slow and fast axes, respectively. The SLM peak wavelength ( $k=420$ ) as a function of the axial strain is also shown in Fig. 6, which exhibits a blueshift with an axial strain sensitivity of  $1.9437 \times 10^{-2}$  nm/ $\mu\epsilon$ .

When an axial strain is applied on a section of the PMF including the PMFBG, the wavelength spacing between the neighboring SLM interference peaks can be expressed from Eqs. (3) and (8) as

$$\begin{aligned} \Delta\lambda_k(\epsilon) &= \lambda_{k-1}(\epsilon) - \lambda_k(\epsilon) \approx \frac{lB(0) + l\epsilon[B(0) - 2c_0]}{k^2} \\ &= \Delta\lambda_k(0) + \delta[\Delta\lambda_k(\epsilon)]. \end{aligned} \quad (10)$$

It is obvious from Eq. (10) that different interference orders have different wavelength spacings. Both the length of the strain-applying PMF and the interference order number determine the wavelength spacing of the neighboring SLM interference peaks. Therefore, the values of the fiber length or the interference order, which are experimentally selectable, can be used to change the output transmission properties, in which the change in the fiber length is easier to achieve due to the fact that a change in the interference order will result in different operating wavelengths, which may result in the change in light source. The value of  $\delta[\Delta\lambda_k(\epsilon)] = (d^2\lambda_k/d\epsilon dk)\Delta\epsilon\Delta k$  during a strain change of  $1000\mu\epsilon$  for a stress-applying fiber length of 40 cm is  $-4.0 \times 10^{-13}$  m, which indicates that the wavelength difference (0.4 pm) of the neighboring maxima cannot be resolved by the OSA (maximum wavelength resolution 50 pm); thus a comblike transmission has been achieved, where the spectral characteristics can be tuned as a whole without changing the wavelength spacing between the neighboring transmission maxima. On the other hand, a long fiber with a length longer than 5.0 m in this case can be adopted to tune the spectral characteristics as a whole while simultaneously changing the wavelength spacing between the neighboring transmission maxima during the strain change. The possibility in adjusting the fiber length provides an opportunity to satisfy specific applications.

#### IV. CONCLUSIONS

In summary, wavelength control by the use of PMFBG SLM has been demonstrated through polarization and strain tuning. First, the interferometric peak wavelengths of the SLM exhibit blueshifts with the increasing strain in comparison with the redshifts for the Bragg resonance wavelengths of the grating, which provides an opportunity to achieve wavelength selectivity. Second, the pronounced difference in the bandwidths of the resonance peaks of the FBG and that of the interferometric peak of the SLM, as well as their tunability, offer a possibility to achieve an easy switching from a narrow PMFBG filter to a SLM comb filter realized by polarization control. Third, the possible selectivity in the values of the fiber length and the interference order provides a method to control the wavelength spacing of the comb filter. Furthermore, in addition to the versatility in the selection of the Bragg wavelength of a FBG and the interferometric peaks of a loop mirror to satisfy specific applications, the realization of the technique on a standard PANDA fiber provides a simple and low-cost approach, which is compatible with the existing fiber-optic systems.

#### ACKNOWLEDGMENTS

This work has been supported by the Natural Sciences and Engineering Research Council of Canada (NSERC), Canada Research Chairs Program, Canada Foundation for

Innovation, the Province of Newfoundland and Labrador, and the Memorial University of Newfoundland.

- <sup>1</sup>M. G. Kuzyk, *Polymer Fiber Optics: Materials, Physics, and Applications* (CRC, Boca Raton, FL, 2006).
- <sup>2</sup>M. K. Davis, G. Ghislotti, S. Balsamo, D. A. S. Loeber, G. M. Smith, M. H. Hu, and H. K. Nguyen, *IEEE J. Sel. Top. Quantum Electron.* **11**, 1197 (2005).
- <sup>3</sup>X. Fang and R. O. Claus, *Opt. Lett.* **20**, 2146 (1995).
- <sup>4</sup>G. Sun, D. S. Moon, A. Lin, W.-T. Han, and Y. Chung, *Opt. Express* **16**, 3652 (2008).
- <sup>5</sup>X. Shu, S. Jiang, and D. Huang, *IEEE Photonics Technol. Lett.* **12**, 980 (2000).
- <sup>6</sup>R. Szipöcs, A. Köházi-Kis, P. Apai, E. Finger, A. Euteneuer, and M. Hofmann, *Appl. Phys. B: Lasers Opt.* **70**, S63 (2000).
- <sup>7</sup>E. G. Turitsyna, R. Bhambher, V. K. Mezentsev, A. Gillooly, J. Mitchell, and S. K. Turitsyn, *Opt. Fiber Technol.* **11**, 202 (2005).
- <sup>8</sup>A. V. Okishev, C. Dorrer, V. I. Smirnov, L. B. Glebov, and J. D. Zuegel, *Opt. Express* **15**, 8197 (2007).
- <sup>9</sup>H.-G. Yu, Y. Wang, Q.-Y. Xu, and C.-Q. Xu, *J. Lightwave Technol.* **24**, 1903 (2006).
- <sup>10</sup>D. S. Moon, B. H. Kim, A. Lin, G. Sun, W.-T. Ham, Y.-G. Han, and Y. Chung, *Opt. Express* **15**, 8371 (2007).
- <sup>11</sup>A. N. Starodumov, L. A. Zenteno, D. Monzon, and E. De La Rosa, *Appl. Phys. Lett.* **70**, 19 (1997).
- <sup>12</sup>D.-H. Kim and J. U. Kang, *Opt. Express* **12**, 4490 (2004).
- <sup>13</sup>J. Xia, P. T. Beyersdorf, M. M. Fejer, and A. Kapitulnik, *Appl. Phys. Lett.* **89**, 062508 (2006).
- <sup>14</sup>S. Kim and J. U. Kang, *IEEE Photonics Technol. Lett.* **16**, 494 (2004).
- <sup>15</sup>L. Men, P. Lu, and Q. Chen, *Electron. Lett.* **45**, 402 (2009).
- <sup>16</sup>M. P. Fok, K. L. Lee, and C. Shu, *IEEE Photonics Technol. Lett.* **17**, 1393 (2005).
- <sup>17</sup>L. Men, P. Lu, and Q. Chen, *J. Appl. Phys.* **103**, 053107 (2008).
- <sup>18</sup>X. Shu, L. Yu, D. Zhao, L. Zhang, K. Sugden, and I. Bennion, *J. Opt. Soc. Am. B* **19**, 2770 (2002).
- <sup>19</sup>J. Noda, K. Okamoto, and Y. Sasaki, *J. Lightwave Technol.* **4**, 1071 (1986).
- <sup>20</sup>K. O. Hill, in *Handbook of Optics IV*, edited by M. Bass, J. M. Enoch, E. W. V. Stryland, and W. L. Wolfe (McGraw-Hill, New York, 2001).